SLAS Discovery 29 (2024) 100164

Contents lists available at ScienceDirect

SLAS Discovery

journal homepage: www.elsevier.com/locate/slasd

A high-throughput cell-based screening method for Zika virus protease inhibitor discovery

Paulina Duhita Anindita [a,b,1], Yuka Otsuka [c,1], Simon Lattmann [b,1], Khac Huy Ngo [a,b], Chong Wai Liew [b], CongBao Kang [d], Reuben S. Harris [e,f], Louis Scampavia [c], Timothy P. Spicer [c,*], Dahai Luo [a,b,g,*]

[a] Lee Kong Chian School of Medicine, Nanyang Technological University, Singapore, Singapore
[b] NTU Institute of Structural Biology, Nanyang Technological University, Singapore, Singapore
[c] Department of Molecular Medicine, The Herbert Wertheim UF Scripps Institute for Biomedical Innovation & Technology, FL, United States
[d] Experimental Drug Development Centre, Agency for Science, Technology and Research (A*STAR), Singapore, Singapore
[e] Department of Biochemistry and Structural Biology, University of Texas Health San Antonio, San Antonio, Texas, United States
[f] Howard Hughes Medical Institute, University of Texas Health San Antonio, San Antonio, Texas, United States
[g] National Centre for Infectious Diseases, Singapore, Singapore

ARTICLE INFO

Keywords:
Zika virus
HTS
Cell-based assay
Protease inhibitors

ABSTRACT

Zika virus (ZIKV) continues to pose a significant global public health threat, with recurring regional outbreaks and potential for pandemic spread. Despite often being asymptomatic, ZIKV infections can have severe consequences, including neurological disorders and congenital abnormalities. Unfortunately, there are currently no approved vaccines or antiviral drugs for the prevention or treatment of ZIKV. One promising target for drug development is the ZIKV NS2B-NS3 protease due to its crucial role in the virus life cycle. In this study, we established a cell-based ZIKV protease inhibition assay designed for high-throughput screening (HTS). Our assay relies on the ZIKV protease's ability to cleave a cyclised firefly luciferase fused to a natural cleavage sequence between NS2B and NS3 protease within living cells. We evaluated the performance of our assay in HTS setting using the pharmacologic controls (JNJ-40418677 and MK-591) and by screening a Library of Pharmacologically Active Compounds (LOPAC). The results confirmed the feasibility of our assay for compound library screening to identify potential ZIKV protease inhibitors.

1. Introduction

Zika virus (ZIKV) is an enveloped, positive-sense single-stranded RNA virus, predominantly transmitted by mosquitoes from genus *Aedes*. ZIKV infections present a wide range of clinical symptoms, from mild fever, rash, and muscle or joint pain in some individuals, to more severe neurological complications, such as microcephaly in newborns [1] and Guillain-Barré syndrome in adults [2]. In recent decades, ZIKV infection rates have increased, with endemic mosquito-borne transmission observed in tropical and subtropical regions spanning over eighty countries. The 2015 outbreak in Brazil, which subsequently led to widespread infections across South and Central America as well as other regions, propelled ZIKV into the global spotlight. The rapid dissemination of ZIKV and its deleterious outcomes underscore the pressing need for efficacious antiviral therapies and vaccines to tackle the virus and mitigate the burden of ZIKV-associated diseases [3].

The ~10 kb ZIKV genome consists of an open reading frame encoding a single-chain polyprotein precursor which undergoes proteolytic processing of its polyprotein precursor, which comprises ten distinct viral proteins. Three proteins (envelope (E), membrane (M), and capsid (C)] are structural proteins which form viral particles. The remaining seven are non-structural (NS) proteins (NS1, NS2A, NS2B, NS3, NS4A, NS4B, and NS5) which are essential for processing, replication, and assembly of new virions. The proteolytic processing takes place at the endoplasmic reticulum (ER) membrane and is primarily catalysed by the heterodimeric NS2B-NS3 protease. NS3 protease ($NS3_{pro}$) is a serine protease located at the N-terminal part of NS3 (~69 kDa), which also contains a C-terminal superfamily 2 helicase domain.

* Corresponding authors.
E-mail addresses: spicert@ufl.edu (T.P. Spicer), luodahai@ntu.edu.sg (D. Luo).
[1] Equal contribution.

https://doi.org/10.1016/j.slasd.2024.100164
Received 18 March 2024; Received in revised form 3 May 2024; Accepted 23 May 2024
Available online 24 May 2024

NS2B is a small ER integral membrane protein of ~14 kDa that functions as an $NS3_{Pro}$ cofactor [4].

Due to its essential function in ZIKV replication cycle, the NS2B-NS3 protease complex has been presented as an attractive drug target [5]. To date, numerous ZIKV protease inhibitor candidates have been identified, but none have progressed to clinical use due to suboptimal pharmacokinetic properties or insufficient cellular activity [6,7]. Therefore, efforts must continue to identify potent ZIKV protease inhibitors suitable for clinical use. High-throughput screening (HTS) has been used to rapidly identify hit compounds for many viral targets [8-12]. When targeting ZIKV protease, it is crucial to generate an HTS assay that enables prompt measurement of ZIKV protease activity, ideally in its native form, to assess the effectiveness of potential inhibitors. However, the membrane-associated nature of ZIKV NS2B-$NS3_{Pro}$ precludes its expression and purification in a native and active form under detergent-free conditions. The current in vitro protease assays employ NS2B-$NS3_{pro}$ constructs lacking the transmembrane regions of NS2B, potentially deviating from the native conditions of the NS2B-$NS3_{Pro}$ complex. Therefore, to overcome some of these limitations, here we present a bioluminescent cell-based protease assay that utilises ZIKV NS2B-$NS3_{Pro}$ to cleave a cyclically permuted firefly luciferase encoding the NS2B-NS3 cleavage site. Our findings indicate that co-expression of ZIKV NS2B-$NS3_{Pro}$ with a cleavage-activated luciferase substrate enables the endpoint assessment of ZIKV protease activity in living cells. Additionally, we showcase its suitability as a tool for HTS campaigns to assess potential ZIKV protease inhibitors.

2. Materials and methods

2.1. Cells, reagents, and compound library

Human embryonic kidney 293T cell line was grown in DMEM (with High Glucose/ GlutaMAX™/ Sodium Pyruvate/Phenol Red; Gibco 10,569,010) supplemented with 10 % foetal bovine serum (FBS; Gibco 10,437,028) and penicillin/streptomycin (Gibco 15,140,122) at 37 °C in a humidified 5 % CO_2 incubator. Transient transfections were performed with either Lipofectamine 3000 (Invitrogen) or PEI MAX (Polysciences, Warrington, PA, USA) according to the manufacturer's instructions. JNJ-40,418,677 compound was purchased from Cayman Chemicals (Ann Arbor, MI, USA). MK-591 compound was from MedChemExpress (Monmouth Junction, NJ, USA). JNJ-40,418,677 and MK-591 were dissolved in DMSO at 100 mM and 29 mM, respectively. Macrocyclic peptide MI-2110 [13] was provided by Dr. Torsten Steinmetzer (Phillips University Marburg, Germany) at 100 mM in distilled water. The Library of Pharmacologically Active Compounds (LOPAC®1280), a collection of 1280 drugs or drug-like compounds with known mechanisms-of-action, was purchased from Sigma-Aldrich (St. Louis, MO, USA).

2.2. Cloning and mutagenesis

ZIKV NS2B-NS3 polyprotein sequence (GenBank accession number: AEN75265.1; residues: S1367-R2113) fused to a C-terminal FLAG tag was purchased from Twist Bioscience as a synthetic human codon-optimised cDNA sequence and cloned under the CMV promoter of pTwist_CMV_BG_WPRE_BSD-mScarlet expression vector. Truncated alleles of the NS2B-NS3 polyprotein were produced by PCR-mediated deletion mutagenesis. The S135A catalytically deficient alleles were generated by site-directed mutagenesis PCR, substituting the S135 residue from $NS3_{Pro}$ catalytic triad with an Ala-residue. All plasmids were confirmed by DNA sequencing. The cycLuc_ZIKV-NS2B plasmid was generated by *Bam*HI-linearisation of cycLuc_TEVS plasmid, a gift from Dr. Roman Jerala (RRID: Addgene_119,207) [14] and subsequent ligation-independent cloning (LIC) of pre-annealed DNA oligonucleotides coding for the NS2B substrate peptide. The dual luciferase dual_cycLuc_ZIKV-NS2B plasmid was constructed by substituting the NeoR ORF from cycLuc_ZIKV-NS2B plasmid with a 2327-bp PCR-amplified DNA fragment from pGL4.82[hRluc/Puro] (Promega) comprising the hRluc and PuroR ORFs. Sequences and detailed descriptions of the plasmid constructs are shown in Supplementary Data 1–5.

2.3. Immunoblotting

293T cells seeded in 24-well plates were co-transfected with 250 ng dual_cycLuc_ZIKV-NS2B construct and 10 - 40 ng NS2B-NS3 ZIKV protease expression plasmid to initially probe the overexpression levels ZIKV protease variants. In another set of experiments, 293T cells were co-transfected with the dual_cycLuc_ZIKV-NS2B reporter and 5 ng GFP-FLAG (mock) or 20 ng of four different ZIKV protease constructs as well as their respective S135A alleles which have no apparent protease activity. Transfections were equalised to 500 ng per well with an empty pTwist_CMV_BG_WPRE_BSD-mScarlet plasmid. Proteins (4.5 % v/v) derived from a 4-µl aliquot of whole-cell protein lysates utilized in the dual_cycLuc_ZIKV-NS2B assay were separated on a 4–12 % gradient NuPAGE Bis-Tris gel. Subsequently, proteins were electroblotted (30 V, 60 min) onto a 0.2 µm PVDF membrane. The proteins bound to the membrane were detected by immunoblotting using an HRP-conjugated anti-FLAG M2 monoclonal antibody (Sigma-Aldrich). Antibody binding was visualised using WesternBright enhanced chemiluminescence HRP substrate (Advansta, San Jose, CA, USA) and detected by a CCD camera imager (ChemiDoc MP, Bio-Rad, Hercules, CA, USA).

2.4. Adaptation of cycLuc_ZIKV-NS2B reporter to 96-well plate format

293T cells seeded in 24-well plates were co-transfected with 250 ng dual_cycLuc_ZIKV-NS2B and 10 ng construct A ($NS2B_{1–130}$—-$NS3_{FL}$) or C ($NS2B_{46–130}$—-$NS3_{Pro}$) plasmids (Fig. 1). These cells were designated as high luminescence cells ("high"). Alongside, another set of 293T cells designated as low luminescence cells ("low") were co-transfected with 250 ng dual_cycLuc_ZIKV-NS2B and 10 ng empty pTwist_CMV_BG_WPRE_BSD-mScarlet plasmids. On the following day, transfected cells were harvested and seeded at 30,000 cells per well (100 µL) into Corning 96-well white opaque, clear bottom plates. The plates were subsequently incubated for 24 h in a humidified 5 % CO_2 incubator.

A cycLuc_ZIKV-NS2B reporter protease inhibition assay was done by seeding the transfected 293T cells (30,000 cells, 50 µL) into Corning 96-well white opaque, clear bottom plates containing 50 µL serially diluted compounds (40 nM to 20 µM final concentration) or 0.5 % DMSO. The plates were briefly shaken and incubated for 24 h in a humidified 5 % CO_2 incubator.

Luciferase activities were detected using Dual-Glo Luciferase assay system (Promega, Madison, WI; E2940). Briefly, the plates were equilibrated to room temperature (RT) for 30 min. Dual-Glo Luciferase reagent was added at 50 µL per well. After 10 min incubation at RT, firefly luciferase (cycLuc) activities were measured using a Synergy H1 microplate reader (BioTek Instruments, VT, USA). *Renilla* luciferase (Rluc) activity were subsequently measured following addition of Dual-Glo Stop & Glo reagent at 50 µL per well and a 10-min incubation at RT.

2.5. Cell viability assay

293T cells in Corning 96-well clear plates were treated with 40 nM to 20 µM compounds or 0.5 % DMSO as a control. Following a 24-h incubation in a humidified incubator (37 °C, 5 % CO_2), 10 µL cell counting kit-8 (CCK-8, MedChemExpress) solution was added into each well. The plates were incubated for 2 h before measuring the endpoint absorbance at 450 nm using a Synergy H1 microplate reader (BioTek Instruments, Winooski, VT, USA).

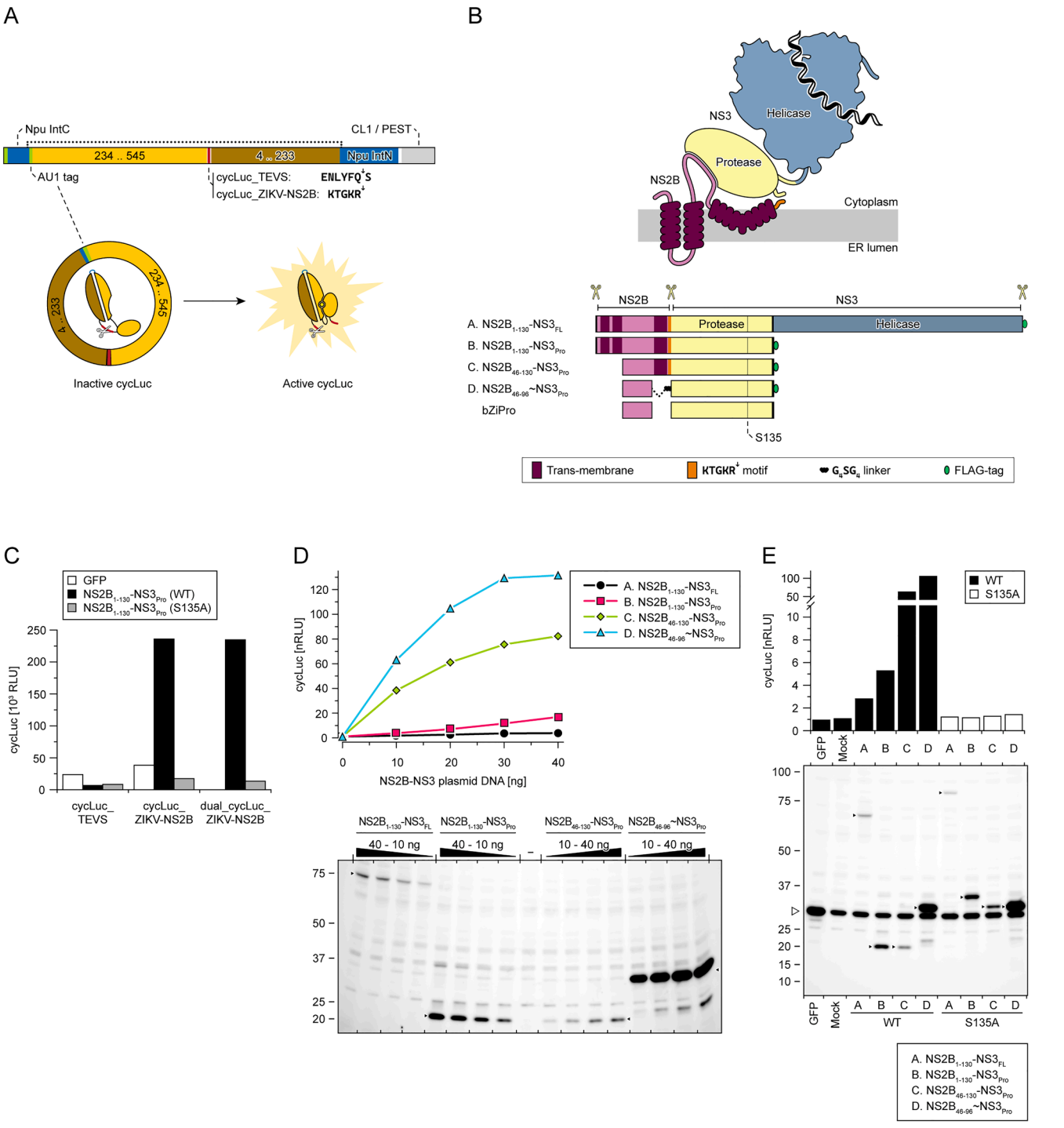

Fig. 1. Design and characterisation of cycLuc_ZIKV-NS2B reporters and ZIKV protease constructs.
A. Schematic representation of the expression and activation of the cyclised circularly permuted firefly luciferase (cycLuc_ZIKV-NS2B) reporter. **B.** Schematic representation of NS2B-NS3 constructs generated in this study. **C.** Activation of cycLuc_ZIKV-NS2B reporters by recombinant ZIKV protease. Various cycLuc reporters were co-expressed with either wild-type or S135A alleles of $NS2B_{1–130}$–$NS3_{Pro}$. Data are representative of two independent experiments performed in a technical singlicate. **D.** Dual_cycLuc_ZIKV-NS2B reporter assay for various ZIKV protease constructs. 293T cells were transfected with 10 - 40 ng plasmid DNA of four different ZIKV protease constructs. Normalised cycLuc activity is shown. Expression levels of various ZIKV protease constructs were probed using Western blot analysis using an anti-FLAG M2 antibody. Filled triangles represent the expected size of each overexpressed ZIKV protease variant. Data are representative of three independent experiments performed in a technical singlicate. **E.** Dual_cycLuc_ZIKV-NS2B reporter assay for various ZIKV protease constructs. 293T cells were co-transfected with the dual_cycLuc_ZIKV-NS2B reporter, 5 ng GFP-FLAG, and 20 ng of four different ZIKV protease constructs. The S135A alleles of respective ZIKV proteases were used as a negative control for protease activity. Normalised cycLuc activity is presented. Expression levels of various ZIKV protease constructs were probed through Western blot analysis using an anti-FLAG M2 antibody. Filled triangles represent the expected size of each overexpressed ZIKV protease variant. Co-transfected GFP-FLAG (open arrow) served as an internal loading control. Data are representative of three independent experiments performed in a technical singlicate.

2.6. Protein expression and purification

Two ZIKV protease constructs [i.e. NS2B cofactor linked with a flexible glycine linker to $NS3_{Pro}$ (gZiPro) and a bivalent construct NS2B cofactor/$NS3_{Pro}$ (bZiPro)], were expressed and purified as previously described with modifications [15]. Briefly, individual construct was transformed into *E. coli* BL21 (DE3) competent cells. The cells were grown in LB broth until the optical density (OD) at 600 nm reached 0.8. Protein expression was induced overnight by addition of 1 mM β-d-1-thiogalactopyronoside at 18 °C. The cells were harvested by centrifugation at 4000 rpm at 4 °C for 30 min. Thereafter, the cells were re-suspended in lysis buffer containing 20 mM HEPES pH 8.0, 500 mM NaCl, 20 mM imidazole, 5 % glycerol, and 2 mM β-mercaptoethanol and passed through GEA Lab Homogenizer PandaPLUS 2000 at 1000 bar (GEA, Germany). The soluble fraction was obtained by centrifugation at 40,000 rpm for 1 h using Ti45 rotor and ultracentrifuge Optima XPN-100 (Beckman Coulter, Brea, CA, USA). Upon soluble fraction loading into a HisTrap HP column (Cytiva, Marlborough, MA, USA), the column was washed with lysis buffer supplemented with 50 mM imidazole. The protein was eluted using elution buffer (20 mM HEPES pH 8.0, 500 mM NaCl, 300 mM imidazole, 5 % glycerol, and 2 mM β-mercaptoethanol). The protein was further purified by size exclusion chromatography using a HiLoad 16/600 Superdex 75 pg column (Cytiva). Eluted protein in fractions were pooled, concentrated, and stored at −80 °C in protein storage buffer containing 20 mM HEPES pH 7.5, 150 mM NaCl, 5 % glycerol, and 2 mM DTT.

2.7. Biochemical protease inhibition assay

Protease activity inhibition by JNJ-40,418,677, MK-591, and MI-2110 was determined in the presence of fluorogenic substrate Bz-Nle-KRR-AMC (Cayman Chemicals). The compounds were serially diluted from 1 mM in an assay buffer (20 mM Tris–HCl pH 8.5, 10 % glycerol, 0.01 % Triton X-100) and 5 μL of each compound concentration was dispensed into wells of a Corning 96-well half-area black plate. The protease (40 μL of 6.25 nM in assay buffer) was subsequently dispensed into each well. The mixture was incubated for 1 h at RT. Subsequently, fluorescence signals from the cleaved substrate were measured upon addition of protease substrate (5 μL, final concentration 10 μM) into the protease-compound mixture using a filter having excitation/emission wavelengths of 340 nm/460 nm at 37 °C at 45 s interval for 30 min in a Synergy H1 microplate reader (BioTek Instruments).

2.8. Bulk transient transfection

Several batches of bulk transfected cells were prepared to ensure consistency across the HTS campaign. The following DNA constructs were sent to Aldevron, USA for scale-up: dual_cycLuc_ZIKV- NS2B plasmids, empty pTwist_CMV_BG_WPRE_BSD-mScarlet plasmid, and $NS2B_{46–130}$—NS3 ZIKV protease expression plasmid. 293T cells were seeded at 9×10^7 cells in 5-Layer Cell Culture flasks (CellPro™). After 24 h incubation at 37 °C with 5 % CO_2, each flask of cells was co-transfected with 115.13 μg of dual_cycLuc_ZIKV-NS2B and 4.61 μg of $NS2B_{46–130}$—NS3 ZIKV protease expression plasmid with 598.68 μg of PEI MAX in 12.5 mL of Opti-MEM. Alongside, empty pTwist_CMV_BG_WPRE_BSD-mScarlet plasmid (4.61 μg per flask) was co-transfected instead of ZIKV protease expression plasmid for the low cells condition. Following a 24-hour incubation at 37 °C with 5 % CO_2, transfected cells were harvested, resuspended in Recovery Cell Culture freezing media (Gibco 12,648,010), and stored in liquid nitrogen.

2.9. Adaptation of cycLuc_ZIKV-NS2B reporter to 1536-well plate format

Frozen transfected cells in cryovials were gradually thawed, resuspended in assay media, and dispensed at 3 μL volumes, achieving a density of 3750 cells per well in an Aurora CWST 1536-well plate (EWB0–42000A). Rows 1–3 were seeded with cells from the low luminescence cell condition while rows 4–48 were seeded with cells from the high luminescence cell condition. Following the addition of 30 nL of test compounds or vehicle to the respective well, plates were incubated for 24 h at 37 °C with 5 % CO_2. The plates were then removed from that environment and allowed to equilibrate at RT for 10 min. Thereafter, 3 μL of Dual-Glo luciferase reagent (Promega E2980) was added per well. cycLuc activity was measured following a 10-min incubation at RT using a PHERAstar FSX (BGM) microplate reader. Subsequently, 3 μL of Dual-Glo Stop & Glo reagents (Promega E2980) were added to each well. Following a 10-min incubation at RT, Rluc activity was quantified.

2.10. Data analysis

Assay quality (Z') and signal-to-background (S/B) ratio were calculated from luminescence signals of high luminescence and low luminescence cells using the following equations:

$$Z' = \frac{3SD \text{ of Low luminescence} + 3SD \text{ of High Luminescence}}{(\text{Low luminescence} - \text{High Luminescence})} \quad (1)$$

$$S/B = \frac{\text{Mean of High luminescence}}{\text{Mean of Low Luminescence}} \quad (2)$$

The protease inhibition response in biochemical protease assay is expressed as the percentage of bZiPro or gZiPro activity. In cell-based protease assay, the response is defined as protease activity, calculated from the percentage of cycLuc activity from treated cells normalised against high and low luminescence cells. IC_{50} values were derived from the sigmoidal dose-response (variable slope) curves. Cell viability was calculated by normalising OD_{450nm} readings from compound-treated cells against those of cell culture medium (0 % cell viability) and OD_{450nm} values of DMSO-treated cells (100 % cell viability). Data normalisation and dose-response curve fitting were performed using GraphPad Prism 10 (GraphPad Software, MA, USA) software.

3. Results

3.1. Construction and validation of the cycLuc_ZIKV-NS2B and dual_cycLuc_ZIKV-NS2B reporters

ZIKV protease activity reporter (cycLuc_ZIKV-NS2B) was constructed based on the cyclically permuted cycLuc_TEVS reporter [14,16]. To generate cycLuc_ZIKV-NS2B, the tobacco etch virus (TEV) protease recognition sequence from cycLuc_TEVS plasmid was substituted with native cleavage site between ZIKV NS2B-NS3 (hereafter referred to as NS2B substrate peptide) (Fig. 1A). Additionally, a dual-luciferase reporter construct (dual_cycLuc_ZIKV-NS2B) for ZIKV protease activity was derived from cycLuc_ZIKV-NS2B by replacing the NeoR open reading frame, under the SV40 promoter, with that of *Renilla* luciferase.

Four candidate variants of the ZIKV NS2B-NS3 complex were designed and evaluated for their potential to specifically cleave and thereby activate the cycLuc_ZIKV-NS2B reporter (Fig. 1B). Construct A ($NS2B_{1–13_0}$-$NS3_{FL}$) encompasses the entire NS2B-NS3 polyprotein and best reflects the ZIKV protease as expressed in the host cells upon viral infection. Construct B ($NS2B_{1–13_0}$-$NS3_{Pro}$) lacks the C-terminal NS3 helicase domain. Construct C ($NS2B_{46–13_0}$-$NS3_{Pro}$) is derived from B and is devoid of two transmembrane helices at the N-terminal region of NS2B. Construct D ($NS2B_{46–9_6}$-$NS3_{Pro}$) is identical to the single-chain gZiPro construct utilised in biochemical protease assay and structural studies of ZIKV NS2B-$NS3_{Pro}$ [17]. It is comprised of the cytosolic NS2B cofactor region (G46-E96) linked to the $NS3_{Pro}$ through an uncleavable nonapeptide Gly4-Ser-Gly4 linker. For all constructs, a catalytic mutant (S135A) of NS3 was generated in parallel to serve as negative controls for protease activity measurement. Finally, additional negative controls for assessment of the cycLuc_ZIKV-NS2B reporters were produced either by transfecting cells with empty vectors or by substituting the ZIKV

protease ORF with that of NeonGreen fluorescent protein (GFP).

To initially assess the efficacy of the newly developed reporters, plasmid DNA encoding wildtype and catalytic-mutant derivatives of construct B was transfected into 293T cells alongside the cycLuc_ZIKV-NS2B reporter plasmid. The expression of catalytically active recombinant ZIKV protease led to the processing of cycLuc_ZIKV-NS2B reporter as evidenced by the considerable increase of the bioluminescence (Fig. 1C). The activation of cycLuc_ZIKV-NS2B reporter, but not cycLuc_TEVS, also demonstrated the selective cleavage of the NS2B substrate peptide by ZIKV protease. On the other hand, the expression of S135A allele of ZIKV protease yielded luminescence levels comparable to control GFP transfections. The observed similarity in basal luminescence levels between cycLuc_TEVS and cycLuc_ZIKV-NS2B reporters indicates that the NS2B substrate peptide is not susceptible to host proteases. Overall, these results substantiate the functionality of the cycLuc_ZIKV-NS2B reporter and its applicability for measuring ZIKV protease activity in 293T cells.

3.2. Dose-dependent response analysis from all protease constructs

We initially tested the co-expression of the dual_cycLuc_ZIKV-NS2B reporter with NS2B-NS3 constructs B and C resulted in a marked increase in the bioluminescence signal (Supp. Fig. 1A). Moreover, the dual_cycLuc_ZIKV-NS2B reporter manifested a sensitivity superior to that of the direct detection by immunoblot. Transfections with as little as 8 ng construct B or C resulted in a more than 8-fold increase of the luminescent signal. At the highest DNA conditions, the dose-response correlation was no longer linear, and saturation was observed. The *Renilla* reporter unveiled a marked reduction of cell viability at and above 25 ng NS2B-NS3 constructs, notably for constructs expressing the full-length NS2B (construct B, Supp. Fig. 1A). Hence, we deemed it is necessary to avoid transfecting cell with more than 50 ng NS2B-NS3 constructs per well under these experimental conditions.

We proceeded to narrow the titration window of the transfected NS2B-NS3 constructs from 10 to 40 ng. We confirmed that for both construct A and B the activation of the cycLuc reporter was correlated linearly with the ZIKV protease expression levels over the whole range tested (Fig. 1D). Constructs C and D showed higher luminescence associated with the protein expression level and tended to saturate already at and above 20 ng NS2B-NS3 constructs. Therefore, to quantitatively compare the differential catalytic activity of all four ZIKV protease constructs, all subsequent experiments were conducted using only 10 ng NS2B-NS3 for transfection (20 ng when immunoblot analysis was conducted).

3.3. Comparison of the protease activity of various ZIKV protease constructs

All four WT NS2B-NS3 constructs manifested substantial catalytic activity, with marked differences in the degree of their activity upon their expression in the cells (Fig. 1E, Supp. Fig. 1B). Cells expressing constructs A and B presented the lowest enzymatic activity with luminescence signals being only a few times higher than that of cells transfected with the control GFP construct. This possibly due to their location on the cell membrane. The N-terminal region of NS2B might be helpful for the orientation of the protease on the cell membrane, which affects the cleavage of the product used in the assay. In stark contrast, cells expressing constructs C and D showed 30-fold increase of luminescence over the basal signal. Looking at the expression levels of the various ZIKV protease forms, it was evident that the higher activity of construct D was merely stoichiometric (Fig. 1E). In contrast, the remaining three constructs were expressed to roughly comparable levels although construct B presented a marginal higher expression than constructs A and C. The apparent molecular weight analysis of all four constructs confirmed the correct self-processing of the single-chain polypeptide at the intervening NS2B-NS3 recognition sequence. When compared to their respective S135A catalytically deficient alleles, WT constructs A, B, and C displayed a reduction in size precisely matching the loss of their NS2B polypeptide chain. Hence, the lack of single-chained precursors for the NS2B-NS3 constructs and the presence of the anticipated polypeptide fragments eliminate the possibility that the observed variations in catalytic activity among the candidate ZIKV protease constructs arise from the expression of malfunctioning proteases. Altogether, we conclude that the dual_cycLuc_ZIKV-NS2B assay serves as a target-specific method to investigate the enzymatic activity of ZIKV protease in living cells.

3.4. Evaluation of dual_cycLuc_ ZIKV-NS2B reporter in 96-well plate format

As a step toward utilising the dual_cycLuc_ZIKV-NS2B reporter in an HTS campaign to identify potential ZIKV protease inhibitors, we optimised and adapted the assay to accommodate a multi-well format as well we assess its robustness and quality. From the four ZIKV protease constructs described above, only constructs A and C were evaluated more extensively here. Construct A was chosen over construct B since it reflects the ZIKV protease as expressed natively by host cells upon infection the best. Construct C was retained because of its high specific activity. Construct D was rejected as its artificial flexible linker may render the catalytic site less accessible to inhibitors and less biologically relevant [17].

We tested the dual_cycLuc_ZIKV-NS2B reporter in 96-well plate format to initially assess assay robustness and quality (Z') as well as signal-to-background ratio (S/B). An assay with Z'>0.5 is rendered as a good assay to be used in HTS [18]. First, we probed the appropriate plasmid quantity which will give cycLuc Z'>0.5 by testing two different plasmid amounts (10 and 25 ng) for each construct in a 24-well plate transfection set-up. Protease activity was determined in 96-well format with cycLuc activity as the read-out. Overall, the variations in the average high signal and low signal from both constructs are minimal across tested plasmid quantities (Supp. Fig. 2A-D). Construct A showed a good cycLuc Z' of 0.69 and a S/B of 4 at 25 ng transfection (Fig. 2A); however, it clearly showed poorer statistics at 10 ng plasmid with a cycLuc Z' of 0.4 and S/B of 3 (Supp. Fig. 2E). On the other hand, construct C showed superior cycLuc Z' of 0.8 and S/B ratio of 35 at 10 ng plasmid and cycLuc Z' of 0.8 and S/B ratio of 27 at 25 ng plasmid (Fig. 2B, Supp. Fig. 2F). cycLuc signals were normalised to Rluc signals, denoted as normalised cycLuc, and the Z' of normalised cycLuc was calculated. We found that the Z' of normalised cycLuc was lower compared to that of the unnormalised cycLuc for both constructs. There was about two-fold reduction in the Z' value of normalised cycLuc (from Z'=0.69 to Z'=0.32) for construct A (Fig. 2A) and such reduction was even more substantial at 10 ng construct A (Supp. Fig. 2E). In contrast, the Z' of normalised cycLuc was 0.55 for construct C (Fig. 2B, Supp. Fig. 2F) which remained within an acceptable range for all tested plasmid quantity. Based on these results, we opted to use construct C for subsequent experiments due to its favourable attributes, including adequate signal dynamic range, excellent Z' for both cycLuc and normalised cycLuc (Z'>0.5), and a high S/B ratio compared to construct A.

3.5. Validation of dual_cycLuc_ ZIKV-NS2B reporter with existing protease inhibitors

We further validated our cycLuc reporter by determining the activity of previously identified ZIKV protease inhibitors, JNJ-40,418,677 and MK-591 [19] as well as MI-2110 [13]. The dose-dependent efficacy of these compounds was confirmed in biochemical protease assay using purified recombinant bZiPro (Fig. 2C, left panel) and gZiPro (Fig. 2C, middle panel) proteases. The protease inhibition activity of these compounds is summarised in Fig. 2C (right panel). Subsequently, cell-based protease activity inhibition by JNJ-40,418,677 and MK-591 was tested in 293T cells co-transfected with construct C and the

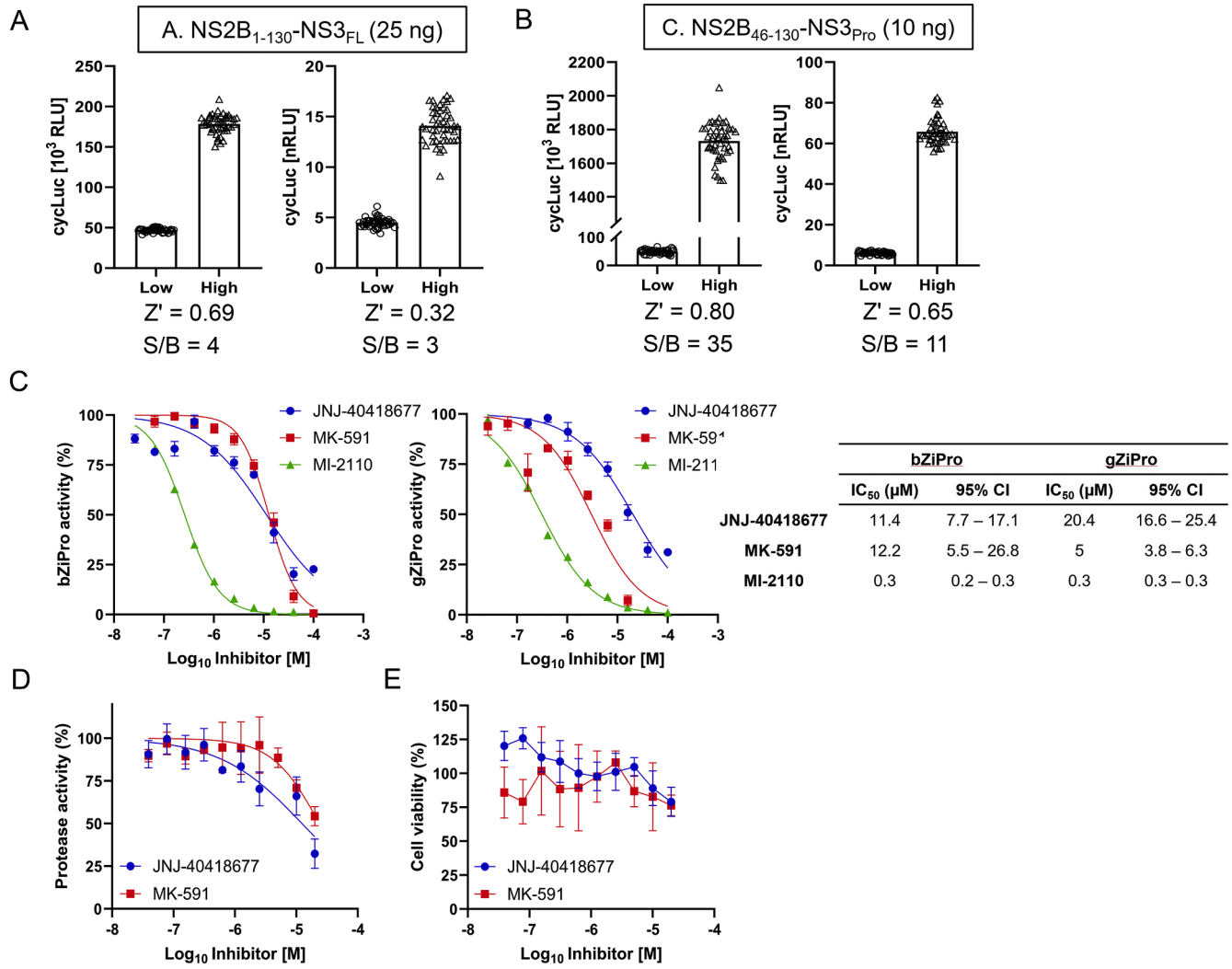

	bZiPro		gZiPro	
	IC_{50} (μM)	95% CI	IC_{50} (μM)	95% CI
JNJ-40418677	11.4	7.7 – 17.1	20.4	16.6 – 25.4
MK-591	12.2	5.5 – 26.8	5	3.8 – 6.3
MI-2110	0.3	0.2 – 0.3	0.3	0.3 – 0.3

Fig. 2. Initial validation of dual cycLuc_ZIKV-NS2B reporter in 96-well plate format.
A. Overall cycLuc and normalised cycLuc activities from low and high luminescence samples. Z' and signal-to-background (S/B) ratios for 25 ng $NS2B_{1–130}$—$NS3_{FL}$ (construct A). **B.** Similar results as in **A** are also shown for 10 ng $NS2B_{46–130}$—$NS3_{Pro}$ (construct C). **C.** Dose-response inhibition curves for JNJ-40,418,677, MK-591, and MI-2110 compounds against recombinant ZIKV proteases bZiPro **(left panel)** and gZiPro **(middle panel)** as determined using biochemical protease assay. Data represent the mean ± SEM ($n = 3$). Summary of IC_{50} and 95 % CI values for JNJ-40,418,677, MK-591, and MI-2110 against bZiPro and gZiPro proteins is shown in right panel. **D.** 293T cells co-transfected with dual_cycLuc_ZIKV-NS2B and $NS2B_{46–130}$—$NS3_{Pro}$ plasmids were treated with serially diluted JNJ-40,418,677 or MK-591. DMSO was used as a control. cycLuc was measured 24 h post-compound treatment using the Dual-Glo® Luciferase assay. **E.** Cytotoxicity of JNJ-40,418,677 and MK-591 on 293T cells as measured using CCK-8 assay. Assays in **(D-E)** were conducted in technical quadruplicates and error bars represent SEM.

dual_cycLuc_ZIKV-NS2B reporter. The two compounds showed partial inhibition against construct C with IC_{50} values of 12.4 μM (95 % CI = 8.3 – 21.0 μM) for JNJ-40,418,677 and 23.7 μM (95 % CI = 17.2 – 50.6 μM) for MK-591 (Fig. 2D). Cytotoxicity, which corresponds to about 25 % decrease in cell viability compared DMSO control, was observed at 20 μM concentration of JNJ-40,418,677 and MK-591 (Fig. 2E). Additionally, we substantiate our choice in using construct C for HTS assay by comparing the protease inhibition from JNJ-40,418,677 and MK-591 against constructs C and D. JNJ-40,418,677 exhibited higher protease inhibition against construct C (membrane associated) in comparison to construct D (cytosolic) although MK-591 showed no difference (Supp. Fig. 3). Therefore, the membrane-associated construct resembling the native ZIKV protease is more suitable for the HTS assay.

3.6. Optimisation of HTS assay in 1536-well plate format and LOPAC screening

We first tested three different cell densities (*i.e.*, 938, 1875 and 3750 cells per well) and compared freshly transfected cells (one day post-transfection, referred to as "cultured") with cell cryopreserved post-transfection (frozen at one day post-transfected and revived days/weeks later for experimentation, referred to as "frozen"). As expected, luminescence signals from both cell conditions exhibited a proportional increase relative to cell densities; however, S/B was achieved best under the condition of 1875 cells per well (Fig. 3A). The cell density of 3750 cells per well showed the best Z' for both cell conditions, with frozen cells demonstrating markedly elevated Z' scores compared to their cultured counterparts (Fig. 3A). Considering these results, as well as practicality, frozen cells were used for subsequent HTS. This approach also ensured homogeneity across experimental iterations.

Next, we investigated the effects of DMSO (0.75 % v/v) on the assay. Overall, 0.75 % DMSO exhibited negligible impact across all tested cell densities and the 3750 cells per well condition showed the least susceptibility to DMSO influence (Fig. 3B). In contrast, the presence of DMSO exerted a substantial impact on the Rluc signal, yielding a consistent 40 % reduction in signal intensity (Supp. Fig. 4A). Subsequently, the assay in 1536-well plate format was validated using JNJ-40,418,677 and MK-591. MK-591 is approximately two-fold less

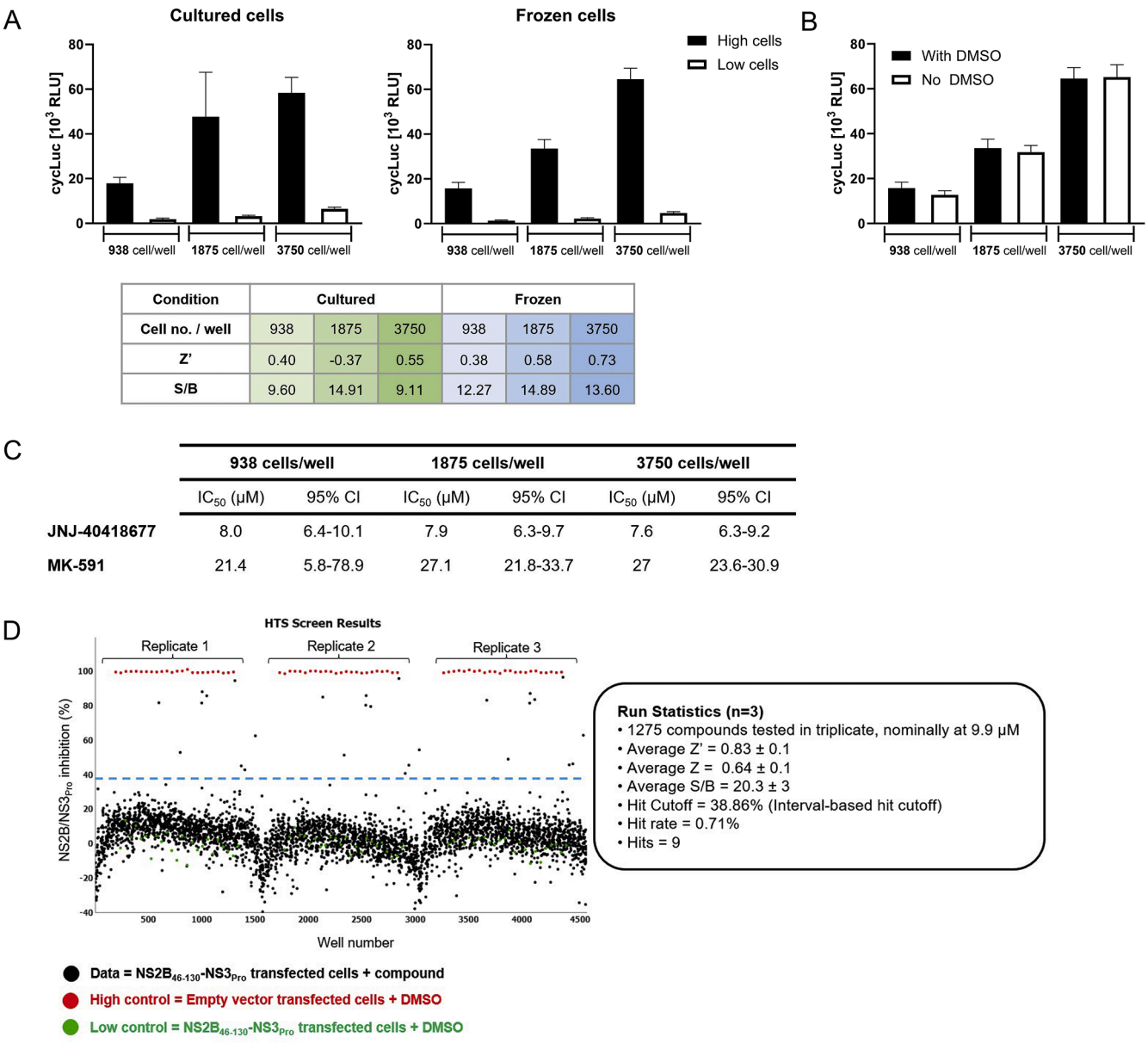

Condition	Cultured			Frozen		
Cell no. / well	938	1875	3750	938	1875	3750
Z'	0.40	-0.37	0.55	0.38	0.58	0.73
S/B	9.60	14.91	9.11	12.27	14.89	13.60

	938 cells/well		1875 cells/well		3750 cells/well	
	IC_{50} (µM)	95% CI	IC_{50} (µM)	95% CI	IC_{50} (µM)	95% CI
JNJ-40418677	8.0	6.4-10.1	7.9	6.3-9.7	7.6	6.3-9.2
MK-591	21.4	5.8-78.9	27.1	21.8-33.7	27	23.6-30.9

Fig. 3. Optimisation of HTS assay in 1536-well plate format and LOPAC screening
A. 1536-well HTS assay with cells from either cultured or frozen conditions, seeded at densities of 938, 1875, and 3750 cells per well. Data represent the mean ± SD of RLU ($n = 40$ wells). **B.** Assessment of 0.75 % v/v DMSO impact on the 1536-well HTS assay under varying cell densities. Data represent the mean ± SD of RLU ($n =$ 24 wells). **C.** Summary of IC_{50} and 95 % CI values for JNJ-40,418,677 and MK-591 against $NS2B_{46–130}$—$NS3_{Pro}$ across various cell densities. **D.** Scatterplot representation of the inhibition efficiency values of the LOPAC compounds against $NS2B_{46–130}$—$NS3_{Pro}$. Black dots represent individual compound values and coloured dots depict the controls. The blue dashed line denotes the 38.86 % inhibition threshold for hits. The screening statistics are summarised in the adjacent box to the graph.

potent than JNJ-40,418,677 (Fig. 2C and Fig. 3C); however, these differences are within the expected range based on prior reports [19]. There is no substantial difference in IC_{50} values between the two compounds across different cell densities (Fig. 3C and Supp. Fig. 4B). From above results, we decided to employ frozen cells at a density of 3750 cells per well for the purpose of conducting HTS.

As a pilot study, we screened the LOPAC library in triplicates at a final nominal concentration of ~10 µM. The assay performance was consistent with an average Z' of 0.83 ± 0.1 and an average S/B of 20.1 ± 3 ($n = 3$ plates) as well as demonstrated good correlation between the replicates (Supp. Fig. 4C). A summary of the pilot screen results is shown in Fig. 3D. A mathematical algorithm was used to identify candidate inhibitor compounds. Three parameters were calculated [1]: the average value for data wells which have values between average – 3SD of the low control and average + 3SD of high control wells [2]; the SD value for the same set of data wells described in expression 1; and [3] the sum of [1] and 3 times of [2] was used as cutoff. Any compound exhibiting greater percent inhibition than the established cutoff parameter was declared as active. Using this "Standard Hit Cutoff" criterion (hit cutoff = 38.86 %), the assay yielded 9 candidate compounds ("hits") and the correlation between plates of this hits is excellent ($R^2 = 0.96$; Supp. Fig 4C). The IC_{50} values of JNJ-40,418,677 and MK-591 fell within the expected range (Supp. Fig. 4D), confirming the suitability and reliability of this assay for larger HTS screening campaign. We also analysed corresponding Rluc read out of this LOPAC screening to assess capability of Rluc signal to evaluate cytotoxicity of compounds. Cytotoxicity shows more diversity in the sample field which demonstrates high sensitivity (Supp. Fig. 5A). However, correlation between cycLuc and Rluc is low, $R^2 = 0.05$ (Supp.

Fig. 5B), indicating high specificity. Most of the hit compounds showed below 40 % cytotoxicity (Supp. Fig. 5B) and thus could be good candidates for further studies.

4. Discussion

The NS2B-$NS3_{Pro}$ complex has emerged as a promising drug target for antiviral intervention due to its central role in the viral life cycle and its high degree of conservation among flaviviruses, which suggests the potential for the development of broad-spectrum antiviral agents, for instance for ZIKV, Dengue virus, and West Nile virus. High-throughput screening campaigns and structure-guided drug design approaches have yielded several promising lead compounds that exhibit potent inhibitory activity against the enzyme in vitro and in cell-based assays. Some of these inhibitors have demonstrated encouraging antiviral efficacy in animal models of ZIKV infection, underscoring their potential as viable therapeutic candidates. However, none of these compounds has been approved for clinical use [19,20].

Many protease inhibitors were screened and evaluated through biochemical assays or developed through computation-based drug design strategies [21-23]. Despite their robustness, those assays do not account for protease's native state in the cells as well as compound's cell permeability. Therefore, a cell-based assay to evaluate the activity of ZIKV protease is more suitable. We chose to develop a cell-based assay utilizing a luciferase-based bioassay due to its considerably enhanced sensitivity and broader dynamic range compared to most alternative reporters. The luciferase as intracellular probe allows for effective implementation at notably lower expression levels than fluorescent proteins, thereby mitigating potential influences on cellular physiology. Employed in either endpoint or real-time non-lytic assays, bioluminescent reporters have proven successful in examining the activity of diverse viral proteases and are amenable to HTS applications [12,24].

In the current study, we designed a cell-based ZIKV protease assay employing cycLuc_ZIKV-NS2B reporter and four different ZIKV protease constructs (Fig. 1A-B). The assay enabled us to monitor ZIKV protease activity in the cells using luciferase signal as a read-out for protease activity. We selected the most suitable protease construct through our assay validation and preliminary transfer to HTS format. We initially narrowed down the construct selection to constructs A and C. Construct A encodes the native full-length NS2B-NS3 protein complex. Construct C encodes an N-terminally truncated NS2B, linked to $NS3_{Pro}$ by its native cleavage site and therefore preserving the natural interaction between NS2B-NS3 protease. Despite being the most biologically relevant construct, construct A failed during the initial assay quality assessment due to very low signal in the assay. Construct C, on the other hand, yielded high luminescence signal with favourable signal dynamics, excellent Z', and S/B ratio. All these characteristics are critical for accurate identification of genuine protease inhibitor during a screening campaign.

We further validated the potency of our cell-based protease assay by assessing its performance against previously identified ZIKV protease inhibitors, namely JNJ-40,418,677 and MK-591 [19]. JNJ-40,418,677 is recognised for inhibiting amyloid beta peptide Aβ42 implicated in Alzheimer's disease [25], while MK-591 is known as an inhibitor of 5-lipoxygenase-activating protein (FLAP) [26]. In our biochemical assays, these two compounds exhibited a dose-dependent protease inhibition against both bZiPro and gZiPro, however, the calculated IC_{50} values differ from those reported in previous studies targeting ZIKV protease [19]. This disparity may arise from the use of different protease constructs between the studies. The compound's binding dynamics with the respective construct might also influence its protease inhibition properties. Comprehensive structural studies are necessary to further clarify this aspect. While both JNJ-40,418,677 and MK-591 demonstrated dose-dependent protease inhibition in our cell-based assay, compound-induced cytotoxicity was also observed at a 20 μM compound concentration. These findings suggest that the ZIKV protease inhibition by these compounds extend beyond ZIKV protease alone by impacting the host cells and concomitantly reducing NS2B-NS3 protease expression levels in the cells. Nonetheless, these results confirm the utility of our cell-based assay system for evaluating protease inhibitor activity.

To finally evaluate whether this assay is applicable to HTS campaigns, we adapted it to a 1536-well plate format and performed a pilot screening using the LOPAC library which is commonly used to help validate new assays. This library represents a panel of drug diversity that typically exhibit a broad range of activity in cell-based and biochemical assays regardless of the target being tested. Many of the compounds in this library are the results of lead optimisation efforts and characterised as marketed drugs, failed development candidates, and "gold standards" that possess well-characterised activities and mode-of-action. The pilot HTS against this library exhibited satisfying Z' with pharmacologic response to the known inhibitors and an acceptable hit rate. Therefore, our developed assay offers a robust and cost-effective strategy to perform HTS campaigns to identify ZIKV protease inhibitors with suitable physicochemical properties such as cell permeability.

CRediT authorship contribution statement

Paulina Duhita Anindita: Writing – review & editing, Writing – original draft, Visualization, Validation, Methodology, Investigation. **Yuka Otsuka:** Writing – review & editing, Writing – original draft, Visualization, Validation, Methodology, Investigation, Formal analysis. **Simon Lattmann:** Writing – review & editing, Writing – original draft, Visualization, Validation, Methodology, Investigation. **Khac Huy Ngo:** Writing – review & editing, Writing – original draft. **Chong Wai Liew:** Writing – review & editing, Resources, Project administration, Conceptualization. **CongBao Kang:** Writing – review & editing, Conceptualization. **Reuben S. Harris:** Writing – review & editing, Funding acquisition, Conceptualization. **Louis Scampavia:** Writing – review & editing, Supervision, Resources, Project administration. **Timothy P. Spicer:** Writing – review & editing, Writing – original draft, Supervision, Project administration, Conceptualization. **Dahai Luo:** Writing – review & editing, Writing – original draft, Supervision, Project administration, Funding acquisition, Conceptualization.

Declaration of competing interest

The authors declare that they have no known competing financial interests or personal relationships that could have appeared to influence the work reported in this paper.

Acknowledgements

This work was supported by National Institute of Allergy and Infectious Disease grant U19-AI171954 and by the Singapore Ministry of Education Academic Research Fund Tier 2 [MOE-T2EP30220–0009]. RSH is an Investigator of the Howard Hughes Medical Institute and the Ewing Halsell President's Council Distinguished Chair at University of Texas Health San Antonio. We thank Dr. Seyed Arad Moghadasi for providing insights on the experimental designs.

Supplementary materials

Supplementary material associated with this article can be found, in the online version, at doi:10.1016/j.slasd.2024.100164.

References

[1] Mlakar J, Korva M, Tul N, Popovic M, Poljsak-Prijatelj M, Mraz J, Kolenc M, Resman Rus K, Vesnaver Vipotnik T, Fabjan Vodusek V, Vizjak A, Pizem J, Petrovec M, Avsic Zupanc T. Zika virus associated with microcephaly. N Engl J Med 2016;374:951–8.

[2] Carod-Artal FJ. Neurological complications of Zika virus infection. Expert Rev Anti Infect Ther 2018;16:399–410.

[3] Pielnaa P, Al-Saadawe M, Saro A, Dama MF, Zhou M, Huang Y, Huang J, Xia Z. Zika virus-spread, epidemiology, genome, transmission cycle, clinical manifestation, associated challenges, vaccine and antiviral drug development. Virology 2020;543:34–42.
[4] van den Elsen K, Chew BLA, Ho JS, Luo D. Flavivirus nonstructural proteins and replication complexes as antiviral drug targets. Curr Opin Virol 2023;59:101305.
[5] Kang C, Keller TH, Luo D. Zika virus protease: an antiviral drug target. Trends Microbiol 2017;25:797–808.
[6] Bernatchez JA, Tran LT, Li J, Luan Y, Siqueira-Neto JL, Li R. Drugs for the treatment of Zika virus infection. J Med Chem 2020;63:470–89.
[7] Li K, Ji Q, Jiang S, Zhang N. Advancement in the development of therapeutics against Zika virus infection. Front Cell Infect Microbiol 2022;12:946957.
[8] Moghadasi SA, Esler MA, Otsuka Y, Becker JT, Moraes SN, Anderson CB, Chamakuri S, Belica C, Wick C, Harki DA, Young DW, Scampavia L, Spicer TP, Shi K, Aihara H, Brown WL, Harris RS. Gain-of-signal assays for probing inhibition of SARS-CoV-2 M(pro)/3CL(pro) in living cells. mBio 2022;13:e0078422.
[9] Mediouni S, Mou H, Otsuka Y, Jablonski JA, Adcock RS, Batra L, Chung DH, Rood C, de Vera IMS, Rahaim Jr R, Ullah S, Yu X, Getmanenko YA, Kennedy NM, Wang C, Nguyen TT, Hull M, Chen E, Bannister TD, Baillargeon P, Scampavia L, Farzan M, Valente ST, Spicer TP. Identification of potent small molecule inhibitors of SARS-CoV-2 entry. SLAS Discov 2022;27:8–19.
[10] Spicer TP. Drug discovery targeting COVID-19. SLAS Discov 2020;25:1095–6.
[11] Smith E, Davis-Gardner ME, Garcia-Ordonez RD, Nguyen TT, Hull M, Chen E, Baillargeon P, Scampavia L, Strutzenberg T, Griffin PR, Farzan M, Spicer TP. High-throughput screening for drugs that inhibit papain-like protease in SARS-CoV-2. SLAS Discov 2020;25:1152–61.
[12] Smith E, Davis-Gardner ME, Garcia-Ordonez RD, Nguyen TT, Hull M, Chen E, Yu X, Bannister TD, Baillargeon P, Scampavia L, Griffin P, Farzan M, Spicer TP. High throughput screening for drugs that inhibit 3C-like protease in SARS-CoV-2. SLAS Discov 2023;28:95–101.
[13] Braun NJ, Quek JP, Huber S, Kouretova J, Rogge D, Lang-Henkel H, Cheong EZK, Chew BLA, Heine A, Luo D, Steinmetzer T. Structure-based macrocyclization of substrate analogue NS2B-NS3 protease inhibitors of Zika, west nile and dengue viruses. ChemMedChem 2020;15:1439–52.
[14] Fink T, Lonzaric J, Praznik A, Plaper T, Merljak E, Leben K, Jerala N, Lebar T, Strmsek Z, Lapenta F, Bencina M, Jerala R. Design of fast proteolysis-based signaling and logic circuits in mammalian cells. Nat Chem Biol 2019;15:115–22.
[15] Zhang Z, Li Y, Loh YR, Phoo WW, Hung AW, Kang C, Luo D. Crystal structure of unlinked NS2B-NS3 protease from Zika virus. Science 2016;354:1597–600.
[16] Kanno A, Yamanaka Y, Hirano H, Umezawa Y, Ozawa T. Cyclic luciferase for real-time sensing of caspase-3 activities in living mammals. Angew Chem Int Ed Engl 2007;46:7595–9.
[17] Phoo WW, Li Y, Zhang Z, Lee MY, Loh YR, Tan YB, Ng EY, Lescar J, Kang C, Luo D. Structure of the NS2B-NS3 protease from Zika virus after self-cleavage. Nat Commun 2016;7:13410.
[18] Zhang JH, Chung TD, Oldenburg KR. A simple statistical parameter for use in evaluation and validation of high throughput screening assays. J Biomol Screen 1999;4:67–73.
[19] Abrams RPM, Yasgar A, Teramoto T, Lee MH, Dorjsuren D, Eastman RT, Malik N, Zakharov AV, Li W, Bachani M, Brimacombe K, Steiner JP, Hall MD, Balasubramanian A, Jadhav A, Padmanabhan R, Simeonov A, Nath A. Therapeutic candidates for the Zika virus identified by a high-throughput screen for Zika protease inhibitors. Proc Natl Acad Sci USA 2020;117:31365–75.
[20] Li JQ, Deng CL, Gu D, Li X, Shi L, He J, Zhang QY, Zhang B, Ye HQ. Development of a replicon cell line-based high throughput antiviral assay for screening inhibitors of Zika virus. Antiviral Res 2018;150:148–54.
[21] Pathak N, Kuo YP, Chang TY, Huang CT, Hung HC, Hsu JT, Yu GY, Yang JM. Zika Virus NS3 protease pharmacophore anchor model and drug discovery. Sci Rep 2020;10:8929.
[22] Santos LH, Rocha REO, Dias DL, Ribeiro B, Serafim MSM, Abrahao JS, Ferreira RS. Evaluating known Zika virus NS2B-NS3 protease inhibitor scaffolds via in silico screening and biochemical assays. Pharmaceuticals (Basel) 2023:16.
[23] Mirza MU, Alanko I, Vanmeert M, Muzzarelli KM, Salo-Ahen OMH, Abdullah I, Kovari IA, Claes S, De Jonghe S, Schols D, Schinazi RF, Kovari LC, Trant JF, Ahmad S, Froeyen M. The discovery of Zika virus NS2B-NS3 inhibitors with antiviral activity via an integrated virtual screening approach. Eur J Pharm Sci 2022;175:106220.
[24] Xie X, Zou J, Shan C, Yang Y, Kum DB, Dallmeier K, Neyts J, Shi PY. Zika virus replicons for drug discovery. EBioMedicine 2016;12:156–60.
[25] Gijsen HJM, Bischoff FP. Chapter five - secretase inhibitors and modulators as a disease-modifying approach against alzheimer's disease. In: Desai MC, editor. Annual reports in medicinal chemistry. Academic Press; 2012. p. 55–69.
[26] Park MS, Sohn MH, Kim KE, Park MS, Namgung R, Lee C. 5-Lipoxygenase-activating protein (FLAP) inhibitor MK-0591 prevents aberrant alveolarization in newborn mice exposed to 85% oxygen in a dose- and time-dependent manner. Lung 2011;189:43–50.